

*EVS29 Symposium
Montréal, Québec, Canada, June 19-22, 2016*

Effect of stator segmentation and manufacturing degradation on the performance of IPM machines, using iCARE[®] electrical steels

Jan Rens¹, Sigrid Jacobs², Lode Vandenbossche¹, Emmanuel Attrazic³

¹*ArcelorMittal Global R&D Gent, J.Kennedylaan 3, 9060 Zelzate, Belgium*

²*(corresponding author) ArcelorMittal Global R&D, J. Kennedylaan 51, 9042 Gent, Belgium,*

sigrid.jacobs@arcelormittal.com

³*ArcelorMittal St Chély d'Apcher, Route du Fau de Peyre, 48200 St Chély d'Apcher, France*

Summary

In order to increase the performance of permanent magnet electrical machines and/or reduce cost, improved manufacturing techniques are continuously being searched for by machine designers. Segmenting the stator core offers the possibility to simplify the winding process, to increase slot fill factor or to minimise wastage of electrical steel. This paper investigates some of the benefits that can be gained from stator segmentation, and highlights the effect of magnetic degradation due to the increased requirement on punching, through a series of finite element models.

Keywords: Efficiency, motor design, power density, permanent magnet motor, materials

1 Introduction

The design choice made for traction electrical machines has a significant influence on its final production cost and performance. With regards to the production of the stator core, recent publications have demonstrated the potential advantages of a segmented approach, where the stator core is assembled from a number of sub-stacks, as demonstrated in Figs 1 (a) to (d) [1-4]. The topology from Fig. 1(a) shows a segment comprising an entire tooth where adjacent segments are interconnected in the back-iron. The topology from Fig. 1(b) shows how individual teeth are inserted into a single annular lamination, whereas Fig 1(c) shows a topology where only the pole-shoes of each tooth are separately inserted in the stator core. Fig 1(d) is a variation on Fig 1(a) for stators with distributed windings and hence a larger number of teeth. It can be understood that each topology offers particular advantages, with the layouts shown in Fig 1(a) and (d) maximising the potential for reducing material wastage as no large stator laminations must be punched, whereas the topologies shown in Fig 1(b) and (c) allowing for the use of pre-fabricated windings to be inserted from, respectively, the outside or inside of the stator core, hence maximising the slot fill factor.

Segmentation of the stator as shown in Fig. 1(a) may lend itself particularly well for electrical machines in automotive applications in order to save on material usage. Further, given the separate production of the rotor and the stator laminations, the air gap width is no longer determined by limitations of the punching tool. There exists therefore a potential to further minimise the gap, compared to when round laminations are used, which can improve the level of the air gap flux, hence torque. And, not in the least, this segmentation approach opens the possibility to use different materials for the rotor and stator core without significantly increasing material cost, which may bring clear benefits due to opposing requirements for the steel in stator

and rotor: for the rotor, an elevated yield stress is imperative to facilitate retention of the magnets, whereas for the stator, the focus lies on using a low-loss material in order to maintain a good efficiency well into high-speed operation. Within the ArcelorMittal electrical steel product range for automotive traction applications called iCARE®, this differentiated approach is included in the steel grades. The Speed grades offer the highest strength level for rotors. The Save and Torque grades offer the lowest losses for the stators, with the Torque grades also providing easier magnetisation behaviour. So, in a segmented design higher rotational speeds, hence compacter machines can be realised, when using Speed for the rotor.

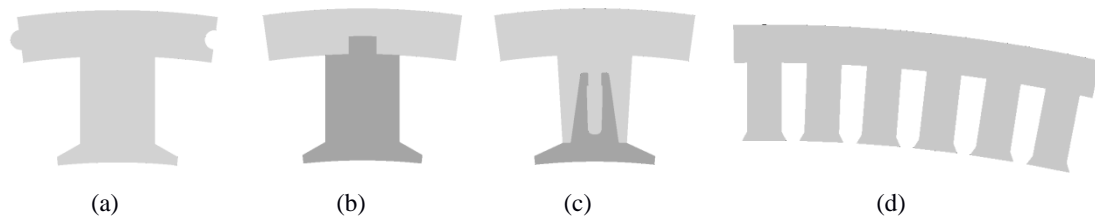


Figure 1: Topologies of stator segmentation, showing a circumferential segment comprising a single tooth (a), a tooth which is radially inserted in an annular yoke (b), plug-in pole-shoes (c) or circumferential segmentation for stators with distributed windings (d)

However, although clear advantages of a segmented approach can be identified, the increased number of sub-stacks that need to be manufactured and assembled may result in a higher influence of material degradation, as the magnetic flux in the stator core is now crossing multiple boundaries between the individual stator segments. Firstly, the increased number of punch-edges is expected to reduce the permeability and increase the core losses of the stator. Further, it is unavoidable that parasitic airgaps exist between adjacent sub-stacks. Additionally, mechanical stresses are likely to be introduced during the final assembly of the sub-stacks, which is especially the case for segmentation arrangements that rely on dovetailed connections to provide stiffness and strength to withstand the pulsating magnetic forces that exist on the stator teeth. For example, for the topology shown in Fig. 1 (c), high stresses and even plastic deformation are expected when the segments are inserted in the teeth [1]. In contrast, stator segments from the topology shown in Fig. 1(a) are pressed together in the stator housing, also inducing significant compressive stresses on the segment interfaces at the yoke, but not requiring tight-fitting dovetailed connections to provide stiffness.

This paper examines the benefits that can be gained from the use of different electrical steels in stator and rotor, as enabled by stator segmentation. Further, the effect of the additional magnetic degradation of the electrical steel that is caused by the additional punching due to segmentation on the machine performance is investigated. The assessment will be made through finite element modelling, starting from a reference model of an Internal Permanent Magnet (IPM) machine and gradually increasing the level of detail in the model. Special attention is paid to iron loss calculations, making use of an advanced methodology that was described elsewhere [5-7]. In the analysis, electrical steels will be used from ArcelorMittal's iCARE® range, which are materials with enhanced properties that are specifically developed for automotive traction machines.

2 Methodology for advanced Iron Loss Calculations

The methodology for the calculation of core losses that is used in the current investigation has previously been developed at ArcelorMittal [5-7]. It is based on finite-element modelling of the electrical machine, where a large number of simulations are run for different timesteps corresponding to a single electrical period. In a post-processing procedure, the resulting waveforms of the magnetic field and polarisation are derived for each mesh element, which allows the prediction of the core losses within each element. This modelling approach relies on measured material data, both for establishing the magnetisation curves that are input to the FE model, as well as for determining material-specific core loss parameters at the specific load-point and conditions that are simulated in the model. For an accurate representation of these material properties, it is indispensable to take measurements over a large range of fields and frequencies, in order to capture the effect of harmonics fields that exist within the machine.

The underlying methodology in the post-processing calculations to derive iron losses is based on an extension of the Bertotti loss model [8], and takes into account the influences of rotational magnetisation and higher harmonic frequencies in the field waveforms, and includes additional fitting parameters which allow to maintain a good accuracy of the loss prediction up to high levels of magnetic polarisation. The equation behind the extended model relies on six material dependent parameters (s_{eddy} , s_{hyst} , s_{exc} , α , β , γ) and is given as:

$$P(J_p, f) = s_{hyst} (1 + (r(J_p) - 1)c) J_p^{(\alpha + \beta J_p)} f_0 + s_{eddy} \sum_{n=1}^{\infty} J_{p,n}^2 (nf_0)^2 + s_{exc} \sum_{n=1}^{\infty} J_{p,n}^{\gamma} (nf_0)^2 \quad (1)$$

taking into account the following definitions:

- s_{eddy} : calculated from electrical conductivity, thickness and mass density of the electrical lamination
- s_{hyst} , s_{exc} , α , β , γ : fitting parameters for the studied electrical steel grade, based on measured Epstein data
- J_p : peak value of the first harmonic component of the magnetic polarisation
- $J_{p,n}$: peak value of the nth harmonic component of the magnetic polarisation
- f_0 : fundamental frequency
- c : local flux-distortion factor, defined as $c = J_{min}/J_p$
- $r(J_p)$: rotational loss factor (empirical loss function, experimentally determined on a few grades)

The extended Bertotti model described above can be used to assess the effects, on the global performance of the electrical machine, that arise from degradation of the electrical steel, caused by elevated temperatures, mechanical stresses, punching or laser cutting. To this effect, it is necessary to conduct additional magnetic measurements that are able to capture the material degradation, and to establish the local magnetisation and loss curves of the degraded material, both as a continuous function of the distance to the cut-edge [5-7]. Within the finite element model, the core geometry is then subdivided in different zones depending on the local degradation of the material, with specific material properties defined for each zone.

In summary, Fig. 2 shows the overall approach that was adopted in this research to calculate iron losses. The geometry of the stator and rotor cores in the Finite Element model was subdivided into different zones, depending on the distance from the cut-edge, in order to establish its effect on the overall performance of the machine. Although the employed iron loss models rely on the output of simulations, using only measurements on materials to provide input data to the models, the approach has previously been validated through comparisons with experimental machine data [7], where it was demonstrated that extending a machine model to include the punch-edge effect gives a better agreement between simulated and measured machine properties.

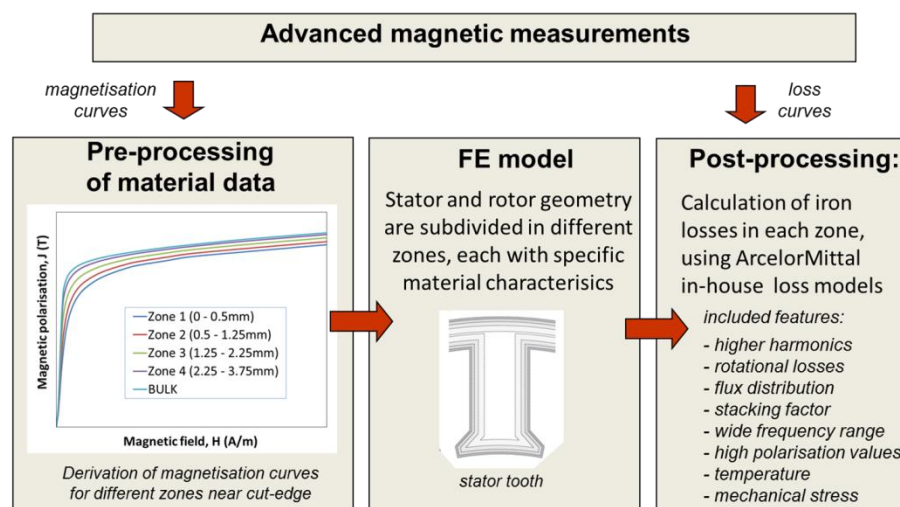


Figure 2: General overview of the numerical scheme of the ArcelorMittal iron loss modelling approach

3 Reference machine model

The machine model shown in Fig. 3 (a) will be used as a reference for further comparisons. It is a 10 pole, 15 slot, interior permanent magnet (IPM) machine, which was designed for an automotive traction application, with specifications shown in Table 1. A fractional slot stator topology with concentrated windings was chosen in order to highlight the potential for stator segmentation. As shown in Fig. 3(b), only 1 pole-pair of the machine is modelled due to symmetry in the geometry. All modelling results in this paper correspond with a nominal operating point where a nominal torque of 100Nm is generated at a rotational speed of 4800rpm (400Hz).

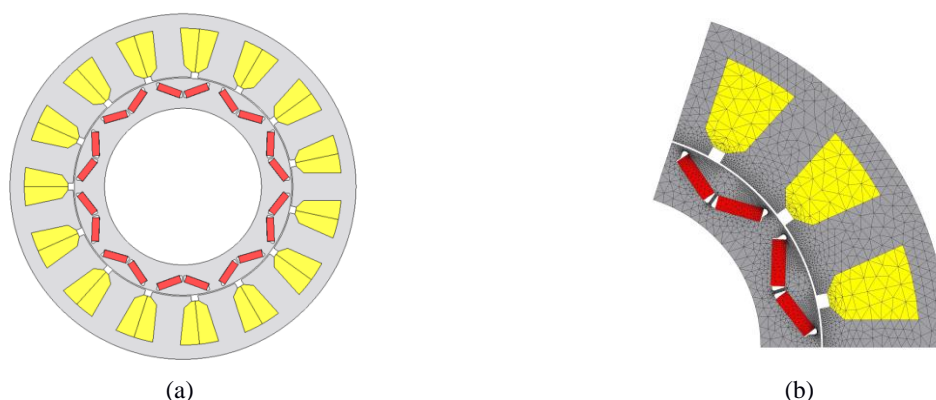


Figure 3: (a) two-dimensional layout of machine and (b) FE model

Table 1: Principal motor specifications

Outer diameter	195mm
Nominal power	50kW
Maximum torque	150Nm
Maximum speed	12000rpm

4 Advantages of using dissimilar materials on rotor and stator

Electrical machines for automotive traction applications are typically designed with a high starting torque capability, and an extended constant power range up to elevated speeds. For the reference IPM machine, these specifications result in conflicting requirements for the rotor and stator laminations: whereas the rotor material should be selected to have a high yield strength to reach high speeds, the stator should preferably be constructed from a steel with high permeability, such that a high flux-density, and hence torque, can be generated. Within its iCARE[®] range of electrical steels for automotive applications, ArcelorMittal has developed a number of steel grades which are specifically optimised to meet given requirements of elevated yield strength, elevated permeability, or low-loss up to high frequencies.

4.1 Materials investigated

The performance of the reference machine is modelled using the following three different electrical steels from the ArcelorMittals iCARE[®] range:

- Save 30-15: an electrical steel with a thickness of 0.3mm, especially designed to reach high efficiencies up to elevated frequencies,
- Torque 30: an electrical steel with a thickness of 0.3mm, especially designed to reach a high permeability and polarisation, and thus allow high torques to be generated
- Speed 35-510 which is designed for a high mechanical yield stress (YS) , and is suitable for high-speed rotors

As the reference machine was originally designed using Save 30-15 in both stator and rotor, a comparison is first made by using Speed 35-510 on the rotor, to take advantage of its elevated yield stress. Then, the replacement of the stator material by Torque 30 is investigated.

4.2 Mechanical design of rotor

As an evaluation will be made of the use of Speed 35-510 instead of Save 30-15 for the rotor material, the geometry of the rotor was re-designed, in order to take into account the elevated yield stress (YS) of Speed 35-510. This increased YS allows the reduction of the rotor structures that are necessary to contain the magnets at high speeds, hence reducing magnetic leakage flux paths. Fig. 4 (a) shows a contour plot of the von Mises stress in a section of the rotor, when the machine is modelled at its maximum overload speed of 12000rpm. where it can be seen that high stress concentrations occur in both rotor bridges X_a and X_b .

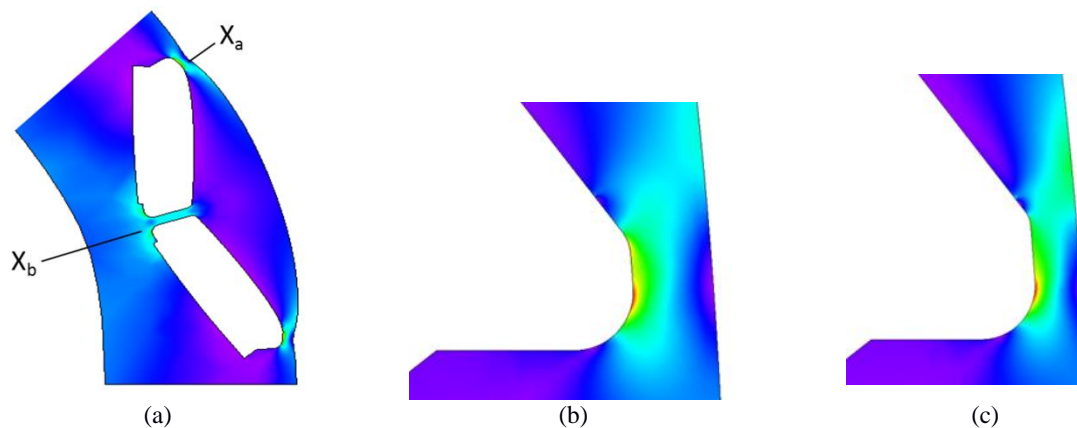


Figure 4 (a): von Mises stress contour plot, superposed on the scaled deformation of the rotor laminations, for a section of the rotor and at maximum speed. The rotor was designed using Save 30-15.

(b) Maximum stress concentration in rotor designed using Save 30-15

(c) Maximum stress concentration in rotor designed using Speed 35-510

During an iterative optimisation of the rotor, both bridge thicknesses X_a and X_b were adjusted simultaneously until a maximum stress was reached of $0.75YS$, to provide some safety margin. This design criterion is based on the assumption that the field load is predominantly (quasi-) static during the lifetime of the IPM. Dynamic loading of the stressed areas can be caused by rotor acceleration and deceleration. If the IPM field application requires a higher resistance against high-cycle dynamic loading the Speed material would provide additional benefits and potential for rotor optimisation as its metallurgical design implies a relatively higher fatigue resistance. Whereas the bridge thickness had originally be designed to be $X_a = X_b = 0.95\text{mm}$ to comply with the YS of Save 30-15, the use of Speed 35-510 resulted in a reduction of both bridges to 0.6mm . Fig. 4 (b) and (c) show a detail of the stress contour plots at the position of maximum stress, at the rotor bridge X_a , for rotors designed with Save and Speed respectively.

As an alternative to re-designing the rotor geometry when the material is changed from Save to Speed, the rotor could be allowed to run at a higher rotational speed, thus requiring a lower torque to reach identical power levels. As an example, when Speed 35-510 is used with the original geometry that was optimised for Save, the rotational speed can be increased from 12000rpm to 13400rpm before the safety margin of $0.75YS$ is reached.

4.3 Comparison of results

The reference motor model was simulated with three combinations of electrical steels, as shown in Table 2. For each combination, the model was set-up with an identical stator geometry and identical input current, whilst the rotor geometry was slightly adapted to take into account the YS of the material, as discussed before. The axial length was adjusted for each model in order to generate an identical torque of 100Nm. Hence, the copper losses are not equal between designs. As the original machine was designed using Save 30-15 on both rotor and stator, the results are given as relative changes from the reference.

Table 2: Relative benefit of using of motor models using different combinations of electrical steel

		model 1	model 2	model 3
Stator steel grade		Save 30-15	Save 30-15	Torque 30
Rotor steel grade		Save 30-15	Speed 35-510	Speed 35-510
Axial length/Active material weight		REF	-5.2%	-6.4%
Losses	Rotor core	REF	+11.1%	+11.6%
	Stator core	REF	-3.4%	-8.8%
	Total loss (Cu + Fe)	REF	-2.5%	-5.9%
Efficiency		REF	+0.1%	+0.2%

As shown in the table, the axial length of the reference machine is reduced by about 5.2% when the high-strength steel Speed 35-510 is used on the rotor, due to the reduced flux leakages paths resulting from the smaller rotor bridges. The reduction in axial length reaches 6.4% if also the high-permeability steel Torque30 is used in the stator. The reduced axial length can be translated directly into a corresponding reduction in mass of copper, steel and permanent magnet material.

In relation to the core losses on the rotor, it can be seen that the replacement of Save 30-15 by Speed 35-510 results in an increase of the losses. This is due to increased hysteresis losses of Speed 35-510, as its microstructure was optimised to a compromise between losses and high-strength, as well as higher eddy-current losses due to the increased lamination thickness compared to Save 30-15. Concerning the stator core losses, it is important to note that the average stator flux-density increases gradually from model 1 through to model 3, due to the improved rotor geometry, as well as the higher permeability of the Torque compared to Save 30-15. This can be seen in Fig. 5, which shows a histogram of the amplitude of polarisation in the stator for all three models. As a result of the increased flux-densities, the loss density is increased somewhat, although the core losses in the stator of model 2 are still reduced by 3.4% due to the reduced stack length. The use of Torque 30 results in an even larger reduction of stator core losses of nearly 9%, due to improved loss characteristics of this material.

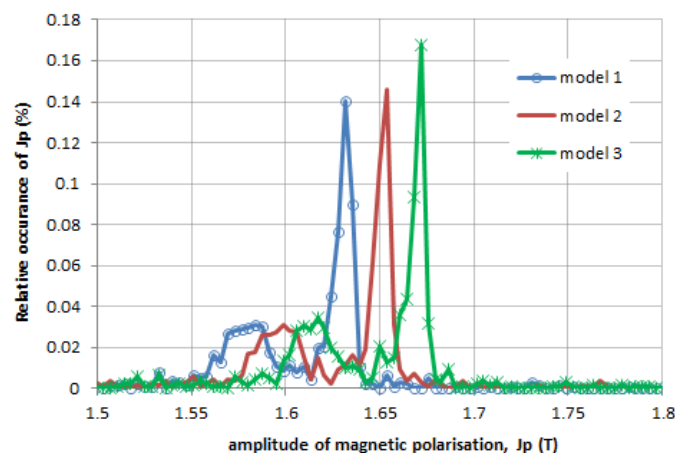


Figure 5: Histogram of J_p in the stator for the three models shown in Table 2. Each histogram shows a double peak behaviour: a lower peak for the yoke polarisation, and a higher peak (1.63T for model 1) for the teeth polarisation amplitude.

To illustrate the origins of the losses on rotor and stator, Figs. 6 (a) and (b) show a break-down of the dynamic losses as a function of the harmonic frequency at which these losses are generated. As can be seen, the rotor losses are mainly caused by multiples of the third harmonic, pointing to the effect of slotting.

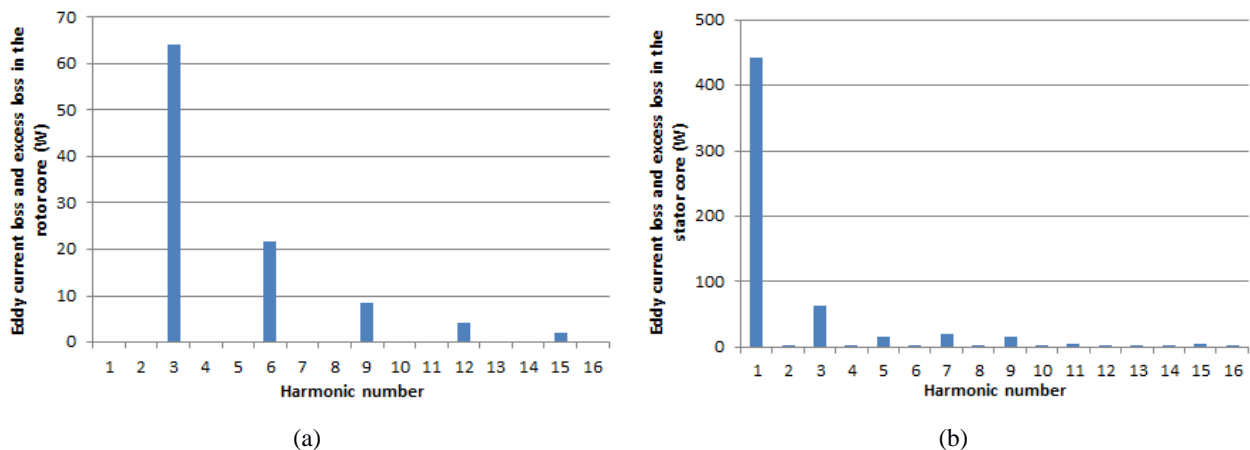


Figure 6: Harmonic content of dynamic losses on the rotor (a) and stator (b) of the machine using Save 30-15 on both rotor and stator. The fundamental frequency equals 400Hz

5 Effect of punching on motor performance

As is described elsewhere [7], the punching process induces plastic deformations and localised stress concentrations in the electrical steel, which can significantly alter the local magnetic properties in the vicinity of the punch edge. Especially for motors with small teeth and fine geometrical features, such localised degradation can considerably impair the performance of the motor and reduce its efficiency. In the current modelling approach, the electrical steel in stator and rotor of the model will be subdivided in a number of zones as a function of the distance to the cut-edge. The material parameters in each zone are determined through a series of laboratory experiments on steel strip.

5.1 Characterisation of material data including cut-edge effect

As the amplitude of degradation and the width of the affected zone are material-dependent parameters, measurements are carried out on both Speed 35-510 and Save 30-15. In principle, the characterisation of the cut-edge effect consists of magnetic measurements on a number of strips which have an identical total width, but which consists of an increasing number of sub-strips, thus gradually increasing the number of cut-edges that are present in the measurement. As the measurements themselves are carried out using an Epstein frame according to international standards IEC 60404-2 and IEC 60404-10, only global material properties are measured, providing data that is averaged over all sub-strips. A further analysis is then carried out to establish the degradation profile as a function of the distance to the cut-edge, for both the magnetisation and loss curves, through the tuning of fitting parameters of pre-described degradation curves [5]. Finally, a number of zones away from the cut-edge are defined, and average material curves are obtained within each zone. For example, Fig. 7a shows the resulting magnetisation curves for Save 30-15 in 5 different zones, whereas Fig. 7(b) shows a comparison of the degradation of the magnetisation curve between Speed 35-510 and Save 30-15, when for each material the zone near the cut-edge is compared with the unaffected material. It can be seen that Save 30-15 in general at moderate and high fields suffers from an increased degradation of the magnetisation curve, compared to Speed 35-510.

The use of an Epstein frame to carry out these measurements, in contrast to earlier studies where a Single Sheet Tester was used [5, 7], has the advantage that the derived curves can be directly introduced in the finite element model, without necessitating an additional correlation from SST to Epstein measurement data. All cuts in the experiments were obtained through shear cutting.

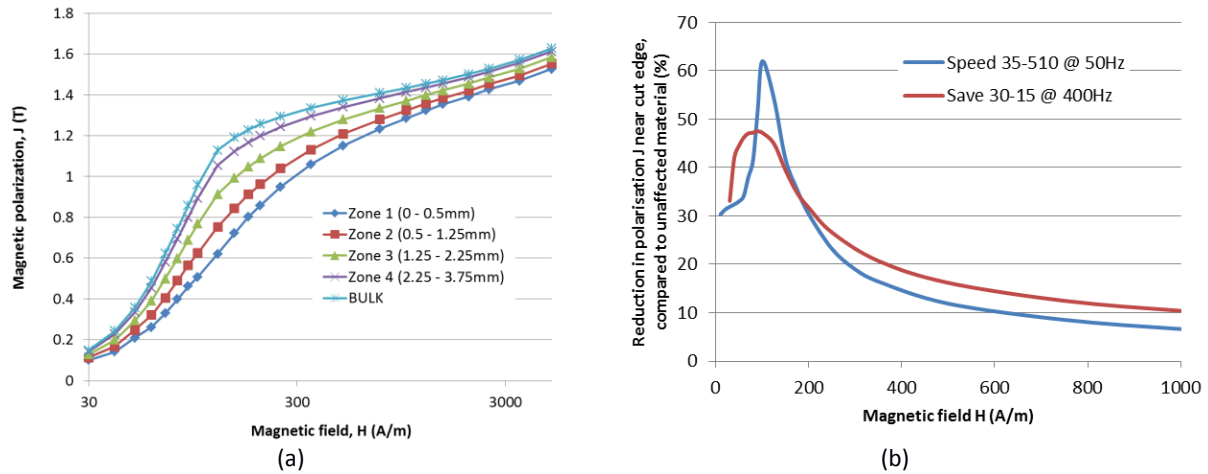


Figure 7 (a): Series of magnetisation curves for Save30-15 for different zones away from the cut edge, where zone1 is on the border of the cut-edge
 (b) Degradation between magnetisation curves of zone 1 compared with the unaffected material, for both Speed 35-510 and Save 30-15

5.2 Model and results

The subsequent simulations to assess cut-edge effects are carried out for Speed 35-510 as rotor and Save 30-15 as stator materials, thus corresponding to model 2 in Table 2. Fig. 8(a) shows the model of the machine, where a total of 5 zones are introduced in both the stator and rotor geometry. As the total degraded region reaches several mm from the cut-edge, the back-iron of the machine is nearly completely affected, whereas the centre of the teeth still contains a large area of unaffected material. To illustrate the effect of the cut-edge on the flux-distribution, Fig. 8(b) shows the flux density through the tooth that is indicated in Fig 8(a) by a dashed line, at time $t=0.2s$, for the models with and without cut-edge effect. It can be seen that the reduced permeability of the zones near the cut-edge results in a shift of the flux density towards the unaffected area of the tooth, hence increasing specific core losses at the centre. Although the areas near the cut-edge conduct less flux, specific core loss may still be increased because of a worsened hysteresis and excess loss behaviour resulting from the material damage. With regards to the rotor, as the majority of the losses are caused by eddy current losses, which are not affected by cut-edge degradation, it is to be expected that punching has a limited effect on rotor losses.

Table 3 gives the results of the simulation with and without cut-edge effect included. It can be seen that the cut-edge effect results in a torque reduction of 2% and an increase in core losses compared to the original performance. In order to facilitate comparison, the table also includes the results of the model with cut-edge, when its axial length is increased to match the original torque of 100Nm. In this case, the core losses would increase with nearly 11% as compared to a machine with unaffected material for equal performance.

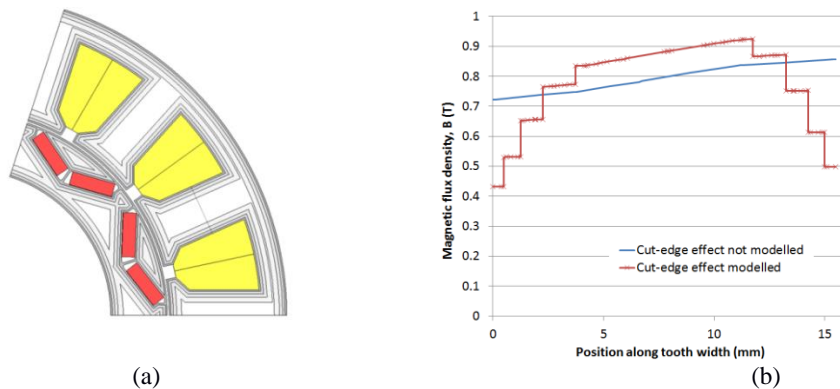


Figure 8 (a): FE model with cut-edge effect included
 (b) Flux-density through a tooth, as indicated on (a) with a dashed line, at time $t=0.2ms$

Table 3: Effect of cut-edge. Results are shown for the case where the axial length of the machine is kept constant, and for the case where the axial length was increased to reach 100Nm.

	Cut-edge not included ,(cf model 2 in Table 2)	Cut-edge included Axial length unchanged	Cut-edge included Axial length adjusted
Rotor steel grade	Save 30-15	Save 30-15	Save 30-15
Stator steel grade	Speed 35-510	Speed 35-510	Speed 35-510
Axial Length (mm)	162.2	162.2	165.7
Torque (Nm)	100	97.9	100.0
P_{total} rotor (W)	121.4	125.2	127.9
P_{total} stator (W)	737.8	807.8	825.1
Total core losses (W)	859.3	933.0	953.0
Efficiency (%) (Cu and core losses)	97.5	97.3	97.3

6 Effect of stator segmentation

As previously discussed, segmentation may degrade the performance of the machine through a number of mechanisms, such as increased mechanical stresses, increased cut-edge length or parasitic airgaps. In the simulations that are presented here, only the effect from the cut-edge and parasitic airgaps are taken into account, ignoring all other aspects which nevertheless could have a significant impact on the machine performance. As a representative length of the parasitic airgap, a value of 50 μ m was chosen [2]. From the candidate segmentation topologies for stators with concentrated windings, Fig 1(a) to (c), the approach using plug-in teeth as shown in Fig. 1(c) has not been modelled as it is likely to result in considerable material degradation due to cutting, mechanical stresses and deformation.

6.1 Homogeneous material properties

Figs 9 (a) and (b) show the models where segmentation was implemented in the yoke and at the root of each tooth, respectively. As can be seen, the cut-edge effect is included on all edges of the rotor and stator geometries. Table 4 shows the simulation results, where each model was simulated for the cases with and without an additional parasitic airgap included. For reference, the model previously shown in Table 3, with cut-edge but without segmentation, against which the effect of segmentation can be compared, is also listed in the table. Finally, for each model, the table shows both the results of the machines with the fixed length of 162.2mm, as well the results when the axial length would be rescaled to reach 100Nm, in order to facilitate comparison between machines with equal performance. In terms of torque density of the machine, it can be noted that the parasitic airgap has the largest negative effect, with a total torque reduction of up to 2.5%. If only the material degradation from the additional punch-edges is considered, the generated torque is nearly unaffected. In terms of losses, firstly it can be noticed that the model with segmentation at the root of each teeth has higher losses compared to the model where segmentation is implemented in the yoke. This is reasonable, given the wider zone of cut-edge degradation, because the width of the tooth is larger compared to the yoke. Further, it can be noted that the consideration of the parasitic airgap results in lower losses, compared to the corresponding model without airgap. The airgap will in effect reduce the inductance and flux-density in the machine, resulting in a lower loss density in the stator yoke.

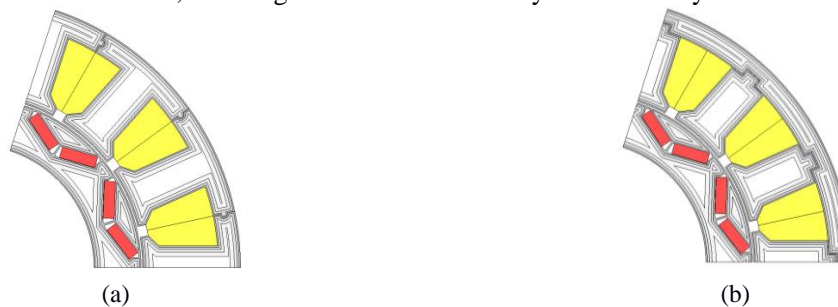


Figure 9: FE model of reference machine with segmented stator, where the segmentation was introduced in the yoke (a) or at the root of the teeth (b)

Table 4: Effect of segmentation. Results are shown for the case where the axial length of the machine was kept constant, and for the case where the axial length was adjusted to reach 100Nm. Cut-edge effect is included in all models.

		No segmentation	Segment at yoke	Segment at tooth	Segment at yoke	Segment at tooth
		Parasitic gap ignored			Parasitic gap included	
L = 162.2mm	Torque (Nm)	97.9	97.8	97.8	95.8	95.5
	P _{total rotor} (W)	125.2	128.4	125.4	124.8	121.3
	P _{total stator} (W)	807.8	814.2	844.8	782.5	795.9
T = 100Nm	L _{100Nm} (mm)	165.7	165.9	165.8	169.3	169.8
	Total losses	1382	1392	1421	1383	1399
	Cu + Fe (W)					

6.2 Taking material anisotropy into account

Although electrical steel that is used in rotating machines is generally of the non-oriented type, there still exists some anisotropy in the magnetic properties when measured in the rolling direction (RD) versus transverse direction (TD). When individual teeth are punched from a sheet, it is important that the teeth are aligned with the easiest direction to magnetise, i.e. in RD, which has favourable magnetic properties. In the previous analysis, this anisotropy was not exploited. In order to include material data in RD and its degradation from cutting, additional Epstein measurements were carried out as described earlier. The simulation results are shown in Table 5, for the model that was shown in Fig 9b, with RD material properties applied in the teeth, whilst for the yoke still the mixed RD-TD data was used as before. It can be concluded that the consideration of anisotropy significantly improves the predicted results, with an overall positive influence of segmentation if the parasitic airgap can be ignored. Accounting for the airgap of 50µm, however, the torque is still reduced by nearly 2% compared to the unsegmented machine, however with an improved efficiency.

Table 5: Effect of segmentation, accounting for anisotropy, for the model with segmentation at the root of teeth (cf. Fig. 9b). Results are shown for the case where the axial length of the machine was kept constant, and for the case where the axial length was adjusted to reach 100Nm. Cut-edge effect is included in all models.

		No segmentation	Parasitic airgap ignored	Parasitic airgap included
L = 162.2mm	Torque (Nm)	97.9	99.2	96.1
	P _{total rotor} (W)	125.2	122.3	118.0
	P _{total stator} (W)	807.8	815.1	767.6
T = 100Nm	L _{100Nm} (mm)	165.7	163.5	168.8
	Total loss (W)	1382	1372	1360

7 Conclusion

Through a series of modelling refinements on a reference machine, the effect of manufacturing and stator segmentation was investigated. Firstly, using ArcelorMittal's iCARE[®] range of electrical steels for automotive applications, it was demonstrated that the use of different electrical steels on the rotor and stator of an IPM motor brings clear benefits for torque density and efficiency of the machine. In particular, the higher yield stress of Speed 35-510 for the rotor material results in a shorter machine, thanks to the increased air-gap flux density, whilst the use of Torque 30 on the stator brings improvements in both axial length and efficiency. In a further simulation refinement, the effect of steel degradation from punching on the overall performance of the machine was quantified. Regarding segmentation, it was shown that the inclusion of parasitic airgaps between the segments of the stator yoke has a significant influence, more than the additional damage to the electrical steel from the increased length of the punched edges. If this airgap could be eliminated, the performance of the machine would actually be improved, thanks to the exploitation of the better magnetic properties of the electrical steel in the rolling direction.

The investigation did not include material degradation due to mechanical stresses that are applied during assembly of the segmented stator, nor the effects of any methods that are used to assemble the substacks, such as interlocking.

References

- [1] J. Richnow et al., *Torque ripple reduction in permanent magnet synchronous machines with concentrated windings and pre-wound coils*, 17th International Conference on Electrical Machines and Systems (ICEMS), 2014
- [2] Z. Q. Zhu et al., *Influence of additional air gaps between stator segments on cogging torque of permanent-magnet machines having modular stators*, IEEE Transactions on Magnetics, Vol. 48, No.6, June 2012
- [3] Kwangyoung Jeong et al., *Measurement and Comparison of Iron Loss in Bonded- and Embossed-Type Segmented Stator Cores for IPMSM*, J Electr Eng Technol Vol 9, No 6, 2014
- [4] K. W. Klontz et al., *Reducing Core Loss of Segmented Laminations*, 2008 SMMA Fall Technical Conference
- [5] Lode Vandenbossche et al., *Impact of cut edges on magnetisation curves and iron losses in e-machines for automotive traction*, EVS25, 2010
- [6] Lode Vandenbossche et al., *Extending the drive range of electric vehicles by higher efficiency and high power density traction motors, via a new generation of Electrical Steels*, EVS26, 2012
- [7] Lode Vandenbossche et al., *Iron Loss modelling which includes the impact of punching, applied to high-efficiency induction machines*, Electric Drives Production Conference (EDPC) 2013
- [8] Bertotti, *General properties of power losses in soft ferromagnetic materials*, IEEE Transactions on Magnetics, 24(1), pp. 621-630, January 1988
- [9] S. Hahlbeck et al., *Design considerations for Rotors with Embedded V-shape Permanent Magnets*, Proceedings of the 2008 International Conference on Electrical Machines, 2008

Authors



Dr. ir. Jan Rens graduated in electromechanical engineering at the University of Leuven. He obtained his PhD in electrical engineering at The University of Sheffield for his research into the design of reciprocating actuators. Later, he held a position as an electrical motor design engineer at Magnomatics Limited. Currently, he works at ArcelorMittal Global R&D Ghent, where he is conducting research on electromagnetic applications of electrical steels.



Ir. Sigrid Jacobs graduated in electro-technical engineering at Ghent University and obtained an MBA at the Vlerick School for management, Belgium. After developing electrical steels at the metallurgy lab of the Ghent university, she joined the ArcelorMittal group and was involved in engineering projects. Now she is portfolio director of the group's R&D activities in Electrical Steels.



Dr. ir. Lode Vandenbossche graduated in electromechanical engineering at Ghent University. He studied the link between magnetic properties and the microstructure of steels at the UGent Electrical Energy Lab, resulting in a PhD about magnetic non-destructive evaluation of material degradation. Currently he works at ArcelorMittal Global R&D Ghent, where he is performing research on electro-magnetic applications and electrical steel solutions.



Emmanuel Attrazic is a superior environment technician. After acquiring production experience in the electrical steel production site of St.-Chély d'Apcher (ArcelorMittal), he joined the plant's metallurgy-quality lab. He further specialised in mechanical and magnetic measurements, beyond the needs of routine production.